Journal of Inflammation Research

Dovepress
Taylor & Francis Group

Open Access Full Text Article

ORIGINAL RESEARCH

Multi-Omics Association Analysis of Mitochondrial Genes in Hypertrophic Scars: Application of Mendelian Randomization

Teng Gong[1,*], Minjuan Wu[2,*], Jiansheng Zheng[3,*], Zhaohong Chen[1]

[1]Burn & Wound Repair Department, Fujian Burn Institute, Fujian Burn Medical Center, Fujian Provincial Key Laboratory of Burn and Trauma, Fujian Medical University Union Hospital, Fuzhou, Fujian, 350001, People's Republic of China; [2]Department of Histology and Embryology, Naval Medical University, Shanghai, 200082, People's Republic of China; [3]Department of Burns and Plastic Surgery, The 909th Hospital, School of Medicine, Xiamen University, Zhangzhou, Fujian, 363000, People's Republic of China

*These authors contributed equally to this work

Correspondence: Zhaohong Chen; Teng Gong, Burn & Wound Repair Department, Fujian Medical University Union Hospital, Fuzhou, Fujian, 350001, People's Republic of China, Email doctorczh@163.com; gtcash@fjmu.edu.cn

Purpose: The role of mitochondrial-related genes in the pathophysiology of hypertrophic scars (HS) is not well understood. This study aims to provide multi-omics insight into mitochondrial genes associated with HS through Mendelian randomization (MR) methods.

Methods: Mitochondrial-related genes in this study were obtained from the MitoCarta3.0 database. Relevant single nucleotide polymorphisms (SNPs) were screened from methylation, expression and protein quantitative trait loci (mQTLs, eQTLs, and pQTLs) of mitochondrial genes. Five regression models including MR-Egger regression, Inverse variance weighted (IVW), Weighted Median, Weighted mode and Simple mode were employed to assess the potential causal relationship between mitochondrial genes and HS risk. Steiger filtering test was used to verify the direction of the causal relationship between genotype, intermediate variables, and final outcomes. Colocalization was employed to identify whether two phenotypes were driven by the same causal variant in a specific region. Multi-omics analysis integrated results from three different gene regulatory layers.

Results: 376 CpG sites, 233 mitochondrial gene expressions and 34 proteins were found associated with HS via MR. Multi-omics results indicated that *HTATIP2* and *PDK1* were genes with tier 1 multi-omics evidence, along with 16 tier 2 genes and 3 tier 3 genes.

Conclusion: This study identified 21 mitochondrial genes with therapeutic potential, with *HTATIP2* and *PDK1* being the most promising genes for clinical application, which may strengthen the understanding of HS pathophysiology.

Keywords: multi-omics, Mendelian randomization, mitochondrial genes, hypertrophic scar

Introduction

Hypertrophic scars (HS) typically occur after burns, surgeries, and extensive injuries, and are a common skin condition caused by abnormal wound healing. They are also a major source of health issues following skin damage.[1–3] The overall prevalence of HS is approximately 32%-72%, with up to 70% of burn patients developing HS, which can significantly impact patients' mental and social well-being and their ability to function, leading to physical issues (such as pain, itching, and loss of joint mobility) and psychological disorders, thereby reducing patients' quality of life and hindering their reintegration into society.[1,4,5] We still do not really understand how HS forms, and currently, there's no one-size-fits-all treatment that works perfectly. Prevention remains the best approach to reduce abnormal scar formation.[4,6,7] Current clinical treatment options include local corticosteroid injections, radiotherapy, laser therapy, and surgical excision,[5,7–9] but the complicated ways HS forms make these treatments less effective in real-life situations.[5,6,10] Additionally, doctors usually diagnose HS just by looking at the symptoms; however, malignant tumors such as dermatofibrosarcoma protuberans may be misdiagnosed as HS, and biopsies are pretty invasive and might affect how HS or tumors

Received: 15 October 2025
Accepted: 26 November 2025
Published: 2 December 2025

develop.[11] In summary, we really need more research to figure out how HS forms in order to develop new treatment and diagnostic methods, identify molecular targets for potential therapies, and achieve the goals of prevention, diagnosis, reduction, and even reversal of HS formation.

Mitochondria are organelles in eukaryotic cells that produce energy, participate in metabolism and signal transduction, and regulate cell growth, differentiation, aging, and death.[12] Previous studies have suggested that the characteristics of HS include ongoing local inflammation, overgrowth of fibroblasts, and excessive deposition of collagen.[13,14] Among these factors, less apoptosis and more fibroblast overgrowth, along with collagen buildup, are linked to changes in mitochondrial function, and directly or indirectly intervening in mitochondrial function could be a potential treatment strategy for HS.[15–19] Many studies on the molecular pathogenesis of HS indicate that chemokines, cytokines, or growth factors play a crucial role in the formation of HS.[7] Mitochondria are key players in infection and inflammation, central to pro-inflammatory responses, participating in the triggering and control of inflammation in diseases, and regulating the function of inflammatory cells and the release of inflammatory factors.[20,21] Additionally, some related mitochondrial genes are also believed to be involved in the process of HS treatment.[15] These studies provide the possibility of targeting mitochondria for HS treatment and show that mitochondrial therapy might be a new option for HS. Although the key role of mitochondria in the pathogenesis of HS has been recognized, specific mitochondrial-related genes and their effects on HS are still not well understood.

Mendelian Randomization (MR) serves as a widely adopted causal inference technique, utilizing genetic variations as instrumental variables (IVs) to handle reverse causation, lessen bias, and enhance the strength of causal inference in studies. These genetic variations are established at conception and are not influenced by later outcomes, diseases, or confounding factors such as socioeconomic conditions, behaviors, or health status.[22–24] The growing data from Genome-Wide Association Studies (GWAS) and molecular quantitative trait loci (QTL) provides a strong foundation for MR research. GWAS utilizes genetic associations based on single nucleotide polymorphisms (SNPs) and traits, which allows researchers to integrate GWAS data with gene expression and methylation data, identifying expression quantitative trait loci (eQTL), methylation quantitative trait loci (mQTL), protein quantitative trait loci (pQTL).[25,26]

Although the role of mitochondria in HS pathology has been noted,[7,20,21] there's still no causal evidence from large-scale population genetic data pointing to specific mitochondrial genes; furthermore, previous studies have rarely integrated methylation, expression, and protein quantitative trait loci (m/e/pQTL) and combined colocalization to improve causal inference and steer clear of linkage and pleiotropy. To address this gap, we are using two-sample Mendelian randomization and combining three layers of QTL evidence with colocalization analysis to better assess the potential causal link between mitochondrial-related genes and HS, providing new avenues for future HS research and possible targets for treatment and diagnosis.

Methods

Study Design

This study is based on a two-sample MR method, using mitochondrial-related genes as exposure variables and HS as an outcome variable. SNPs were used as IVs to explore the causal association between mitochondrial genes and HS based on GWAS data through three levels of analysis: DNA methylation, gene expression, protein abundance. Subsequently, colocalization was used to strengthen causal inference, and Steiger filtering analysis was used to test the direction of causality. Finally, multi-omics analysis was conducted to combine the results from mitochondrial mQTL, eQTL, and pQTL to get a complete picture of how mitochondrial-related gene regulation is linked to HS at various levels (Figure 1). The MR analysis methods used in this study followed the three main assumptions of MR research[27] and the STRIOBE-MR guidelines (Supplementary Table S1).[28]

Data Sources

The mitochondrial-related genes are sourced from the MitoCarta3.0 database, which comprises an updated list of 1136 human mitochondrial genes.[29] The SNP-CpG associations found in blood samples were obtained by McRae et al from DNA mQTLs data in 1980 European individuals.[26] The blood eQTLs dataset was obtained from the eQTLGen

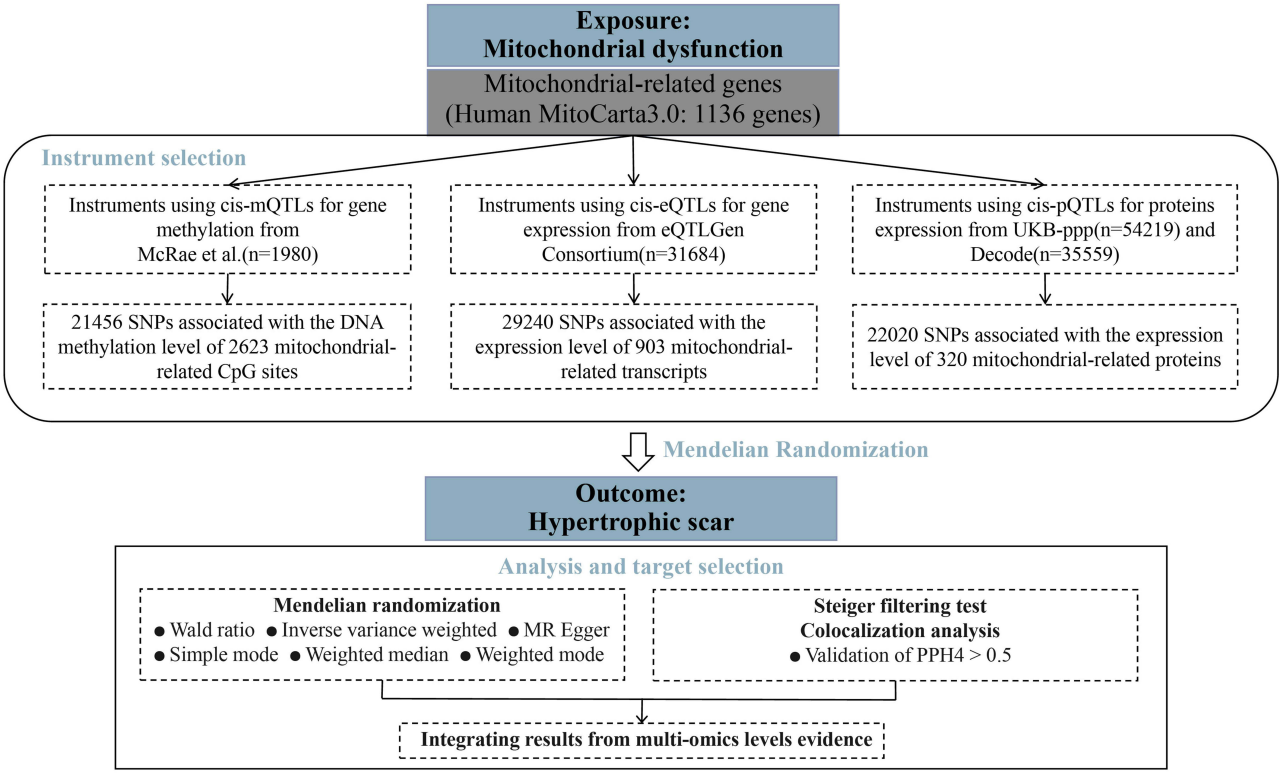

Figure 1 Flow chart.
Abbreviations: QTL, quantitative trait loci; SNP, single nucleotide polymorphisms; PPH4, posterior probability of H4.

consortium (https://www.eqtlgen.org/phase1.html), which comprises 31,684 individuals. The pQTLs were derived from the UK Biobank pharmacoproteomics project (UKB-ppp: https://registry.opendata.aws/ukbppp/) involving 54,219 UKB participants, and a GWAS study (Decode) that measured plasma protein levels in 35,559 Icelanders using 4907 aptamers conducted by Egil Ferkingstad.[30] The genetic association with HS was derived from the FinnGen database (https://www.finngen.fi/fi) (1866 cases and 423,041 controls, dataset number L12_HYPETROPHICSCAR). The website was last accessed on July 15, 2024. The data collected was sourced from European populations (Table 1). The original studies obtained informed consent from the participants, so this part of the study does not need ethics committee approval.

SNPs Selection Criteria

IVs were selected from mitochondrial gene mQTLs, eQTLs, and pQTLs, with a screening criterion of $P < 5\times10^{-8}$, and an F-statistic greater than 10 as an indicator to exclude weak instrumental variables. The Linkage disequilibrium coefficient (r2) was set at 0.3, the linkage disequilibrium region width was set at 500kb and a minor allele frequency (MAF) > 0.01 was set, to ensure the SNPs were independent and to eliminate the impact of linkage disequilibrium on the results.

Table 1 Information of Included Studies and Consortia

Type	Data Source	Sample Size	Cases	Population
mQTLs	McRae et al[26]	1980	–	European
eQTLs	eQTLGen	31684	–	European
pQTLs	UKB-ppp	54219	–	European
pQTLs	Decode[30]	35559	–	European
HS	FinnGen (L12_HYPETROPHICSCAR)	424907	1866	European

Abbreviations: mQTL, methylation quantitative trait loci; eQTL, expression quantitative trait loci; pQTL, protein quantitative trait loci; HS, hypertrophic scar.

https://doi.org/10.2147/JIR.S567534

LDtrait (https://ldlink.nih.gov/?tab=ldtrait) was used to exclude SNPs related to confounding factors and outcomes,[11] and SNPs located within ±1000kb of the cis-regulatory regions of mitochondrial genes were extracted. Relevant IVs were extracted from the mQTLs, eQTLs, and pQTLs data for mitochondrial genes. Relevant SNPs were extracted from the GWAS summary data of the outcome variable (HS), excluding any palindromic SNPs, removing SNPs directly related to the outcome variable (HS) ($P < 5\times10^{-8}$). MR-PRESSO was used to identify and exclude outlier SNPs.

Cis-mQTLs, Cis-eQTLs, and Cis-pQTLs in the Whole Mitochondrial Genome and MR Analysis for HS

The MR-Egger regression, inverse variance weighted method (IVW), weighted median method, weighted mode, and simple mode were five regression models applied in two-sample MR analysis to assess the potential causal relationship between mitochondrial genes and HS risk. IVW served as the primary method for causal estimation, while the other methods were used as supplementary analyses. When SNPs≤3, the effect of a single SNP on the outcome was assessed using the Wald ratio method in conjunction with fixed-effect IVW. When SNPs>3, random-effects IVW was used. In IVW, when estimating causal effects using multiple SNPs as IVs, the inverse of the variance (R^2) for each locus was used as a weight, and the causal effect estimates for each locus were weighted and summed, resulting in the final estimate as the causal effect estimate of the IVW method. MR-Egger essentially relied on a weaker assumption (InSIDE) than IVW to perform causal effect estimation by introducing a regression intercept to detect and correct biases caused by the pleiotropy of IVs. MR-Egger's results were referenced when horizontal pleiotropy was present. The false discovery rate (FDR) served as an indicator of the error rate, and was calculated for *P*-value correction. The formula for calculating FDR is: $FDR = \frac{P_{value}*Rank_{max}}{P_{rank}}$.

Cochran's Q test and I^2 were used to assess the heterogeneity of SNPs. $P < 0.05$ in the Cochran's Q test indicates heterogeneity. The value of I^2 ranges from 0% to 100%, and I^2 >50% indicates a certain degree of heterogeneity in IVW results. The calculation formula is $I^2 = \frac{Q-Q\_df}{Q} \times 100\%$. The MR-Egger method's intercept was used for analyzing pleiotropy, and Leave-one-out was used for sensitivity analysis. The MR-Egger regression intercept and MR-PRESSO were used to detect pleiotropy of SNPs. When the MR-Egger regression intercept and 0 showed no statistical significance ($P > 0.05$) and the MR-PRESSO level pleiotropy test results were not significant ($P > 0.05$), it indicated that SNPs do not have a pleiotropic effect. In the Leave-one-out analysis, each SNP was removed one at a time to observe the impact of each SNP on the results. All MR analyses were conducted using the TwoSample MR package in R version 4.1.0, with a significance level of $\alpha = 0.05$.

Steiger Filtering Analysis

Steiger filtering test was used to check the direction of the causal relationship between genotypes, intermediate variables, and final outcomes. This method is based on the random distribution of genetic variation, looking at how IVs affect intermediate variables and final outcomes, and calculating the correlation between the two to see if the causal direction of the genotype matches for both. This study calculated how much variance was explained by instrumental variable SNPs on mitochondrial gene CpG sites/gene expressions/protein levels and the variance of HS. We also checked whether the variance of HS was smaller than that of the mitochondrial gene CpG sites/gene expressions/protein levels. In the MR Steiger results, if HS's variance is smaller than that of the mitochondrial gene CpG sites/ gene expressions/ protein levels, it's marked as "TRUE", which means the causal relationship lines up with what we expected, while a "FALSE" result means the causal relationship goes against what we expected.

Colocalization Analysis

The colocalization analysis was employed to ascertain whether two phenotypes were influenced by the same causal variant within a designated genomic region, thereby reinforcing the evidence for their association. In this investigation, the underlying assumption of colocalization analysis posited that each trait could have a maximum of one true causal variant in the specified region. Five mutually exclusive model assumptions (H0-H4) delineated all conceivable association scenarios. H0: Phenotype 1 (GWAS) and Phenotype 2 (QTL or GWAS) do not exhibit significant associations with

any SNPs in that genomic region. H1/H2: Either Phenotype 1 or Phenotype 2 demonstrates a significant association with SNPs in the specified genomic region. H3: Both Phenotype 1 and Phenotype 2 show significant associations with SNPs in that genomic area, but these associations arise from distinct causal variant loci. H4: Both Phenotype 1 and Phenotype 2 are significantly associated with SNPs within that genomic region and are driven by the same causal variant locus. In the course of the colocalization analysis, posterior probabilities (PP.H0-PP.H4) were computed for each of the five models, with the cumulative sum of these probabilities equating to 1. A higher posterior probability indicates a greater likelihood that the model assumption is accurate based on the observed data. This study supports the H4 assumption, as the H4 model suggests that both traits are governed by the same causal variant. Generally, a PP.H4 value exceeding 0.5 is regarded as validation of the H4 model assumption.[31] The R package "coloc" was utilized to identify SNPs located within ±1000kb of the cis-regulatory region of mitochondrial genes for the purpose of colocalization analysis. A PP.H4 value greater than 0.7 is interpreted as strong evidence of colocalization between the two traits in the specified region, while a value between 0.5 and 0.7 indicates moderate evidence for their colocalization in that area.

Integrating Results from Multi-Omics Level of Evidence

To comprehensively understand the relationship between mitochondrial-related gene regulation and HS at different levels, this study used multi-omics analysis to integrate results from three different levels of gene regulation. We categorized candidate genes into three tiers: ①Tier 1 genes are those linked to HS at the levels of methylation, gene expression, and protein abundance (FDR<0.05), with gene expression and protein abundance showing the same causal direction with HS; ②Tier 2 genes are those linked to HS at any two of the three levels (FDR<0.05); ③Tier 3 genes are those for which any one of the three levels meets the criteria of being linked to HS (FDR<0.05) and having a colocalization PP.H4>0.5.

Ethical Statement and Human Samples

All human samples were collected after written informed consent was obtained, and the research protocol was approved by the Ethics Committee of Fujian Medical University Union Hospital (approval number: 2025KY428). Hypertrophic scar samples were obtained from patients who underwent scar excision in Fujian Medical University Union Hospital. Normal skin samples were collected from patients who underwent limb amputation in Fujian Medical University Union Hospital.

Cell Isolation and Culture

Following the removal of excess subcutaneous adipose tissue from the skin, the dermal sections were finely minced and subjected to tissue block explant culture to obtain Hypertrophic Scar Fibroblasts (HSFs) and Normal Skin Fibroblasts (NSFs). The fibroblasts were cultured in Dulbecco's Modified Eagle Medium (DMEM) (Gibco, Grand Island, NY, USA) enriched with 10% Fetal Bovine Serum (FBS) (Corning, USA), along with 100 U/mL of penicillin and 100 μg/mL of streptomycin. These cultures were maintained in a humidified incubator set to 37°C with an atmosphere of 5% (v/v) CO2. For subsequent experiments, fibroblasts in the third to fifth passage were utilized.

qRT-PCR

Total RNA was obtained from the dermal layers of both normal skin and hypertrophic scar tissues through the application of Trizol reagent (R0016, Beyotime, Shanghai, China). The synthesis of the first-strand complementary DNA (cDNA) was carried out utilizing HiScript II Reverse Transcriptase (R223-01, Vazyme, Nanjing, China). Subsequently, the mRNA expression levels were assessed via quantitative reverse transcription polymerase chain reaction (qRT-PCR) employing ChamQ SYBR qPCR Master Mix (Q311-02, Vazyme, Nanjing, China). The quantification of mRNA expression was standardized against β-actin RNA. Each reaction was conducted in triplicate on an ABI PRISM 7500 StepOnePlus platform, with data analysis performed following the comparative CT method. The primer sequences used are listed below: HTATIP2-F (5'-TCGTCTTTCAAAGTAATCCTTGAGT-3') and HTATIP2-R (5'-GCGATAATCACAATAGGCAAA-3').

Western Blot

Cell or tissue proteins were extracted using RIPA buffer (NCM Biotech, Suzhou, Jiangsu, China) at a temperature of 4 °C for a duration of 30 minutes. Following this, samples were subjected to centrifugation at 12,000 × g for 15 minutes to facilitate the separation of cellular debris. The concentration of proteins in the resulting supernatant was quantified utilizing a BCA assay kit (Thermo Fisher Scientific, Carlsbad, CA, USA). Subsequently, the proteins within the lysates were resolved via sodium dodecyl sulfate-polyacrylamide gel electrophoresis (SDS-PAGE) and subsequently transferred onto polyvinylidene difluoride (PVDF) membranes (Millipore, Billerica, MA, USA). The membranes were then subjected to a blocking step using QuickBlock Western Blocking Solution (Beyotime, Shanghai, China) for 10 minutes, followed by an overnight incubation with primary antibodies at 4°C. Afterward, the membranes were incubated with horseradish peroxidase (HRP)-conjugated secondary antibodies at room temperature for 1 hour. The primary antibody used was rabbit anti-HTATIP2 (1:1000; Cat. No. ab177961, Abcam, Cambridge, UK), and the corresponding secondary antibody was goat anti-rabbit IgG (Cat. No. ab288151, Abcam, Cambridge, UK). Imaging of the protein bands was conducted using a GE Amersham Imager 600 (GE Healthcare, Little Chalfont, USA), with β-actin serving as an internal control. All experimental procedures were conducted in triplicate to ensure reliability of the results.

Cell Immunofluorescence

The expression levels of HTATIP2 in fibroblasts were assessed via immunofluorescence techniques. Fibroblasts derived from both normal skin and hypertrophic scar tissues were cultured on glass coverslips for a duration of 24 hours. Subsequently, the cells underwent fixation using a 4% paraformaldehyde solution at room temperature (25 °C) for 15 minutes. Following fixation, a blocking step was performed utilizing goat serum at room temperature for 1 hour. The cells were then treated with primary antibodies targeting HTATIP2 (dilution 1:100, Cat. No. ab177961, Abcam, Cambridge, UK) and incubated overnight at 4°C. After that, a secondary antibody (Cat. No. ab150077, Abcam, Cambridge, UK) was applied at room temperature for 2 hours. Lastly, the cells were counterstained with DAPI at room temperature for 5 minutes, and the outcomes were analyzed using a fluorescence microscope.

Results

Results for SNPs Screening

This study screened out 16,091 SNPs associated with 2489 mitochondrial-related DNA methylation CpG sites from cis-mQTL (Supplementary Table S2). From cis-eQTL, 25,928 SNPs linked to the expression of 893 mitochondrial-related transcripts were obtained (Supplementary Table S3). From two proteomic cohort studies' cis-pQTL, 3791 SNPs associated with the expression of 170 mitochondrial-related proteins (137 unique proteins) were identified (Supplementary Table S4).

Mitochondrial Gene Methylation and HS

cis-mQTLs were used as genetic tools for MR analysis to systematically assess the causal effects of mitochondrial genes on HS. Among the 376 CpG sites found to be associated with HS (Supplementary Figure S1), 180 served as protective factors, while 196 were risk factors. The IVW results showed that cg25628542 (*AADAT*) was a protective factor for HS (OR=0.920, 95% CI: 0.877–0.965, $P<0.001$, FDR=0.015). cg17372223 (*NT5DC2*) was also identified as a protective factor for HS (OR=0.937, 95% CI:0.902–0.973, $P<0.001$, FDR=0.015). In contrast, cg11728787 (*HEMK1*) was identified as a risk factor for HS (OR=1.185, 95% CI:1.093–1.285, $P<0.001$, FDR=0.002).cg07434944 (*MRPL23*) was identified as a risk factor for HS (OR=1.319, 95% CI:1.170–1.488, $P<0.001$, FDR<0.001).

When considering the conditions of $P<0.05$ and $I^2>50\%$ in the heterogeneity analysis, it was indicated that cg23811061 from the *IMMT* gene (with $I^2=55\%$, Cochran's Q=35.528, P=0.003) and cg18676053 from the *STOM* gene (with $I^2=53\%$, Cochran's Q=35.832, P=0.005) showed significant heterogeneity. Except for these two, other CpG sites showed no significant heterogeneity.

Based on the analysis using the MR Egger regression intercept, 9 CpG sites near 5 genes were found to be significantly different from 0 ($P<0.05$), specifically those of *MRSA* (cg26077133, cg02319733, cg12940923, cg16038868), *IMMT* (cg06002975, cg23811061), *MRPL23* (cg07578618), *HIBADH* (cg00453374), and *CPT1B* (cg17137457). By MR-PRESSO

analysis, 5 CpG sites near 4 genes revealed significant horizontal pleiotropy: *IMMT* (cg23811061, *P*=0.003), *YBEY* (cg14065109, *P*=0.006), *STOM* (cg18676053, *P*=0.009) and *STOM* (cg14215970, *P*=0.049), and *PDK1* (cg04033559, *P*=0.030). Therefore, excluding these 14 CpG sites, a total of 362 HS-related CpG sites did not show any horizontal pleiotropy, suggesting the MR results from this study were robust (Supplementary Table S5).

Steiger filtering test results showed that all the mitochondrial gene CpG sites in the HS dataset were "TRUE", suggesting that the causal relationship between the mitochondrial gene CpG sites and the outcome aligned with what we expected (Supplementary Table S5).

The colocalization analysis of mQTLs for HS and mitochondrial genes revealed that 4 CpG sites near 2 genes significantly shared causal variants (PP.H4>0.7), including *MRPL23* (cg23135908, PP.H4=0.929) (cg06498964, PP.H4=0.861), (cg07578618, PP.H4=0.712), and *USP30* (cg12535380, PP.H4=0.743) (Supplementary Table S5).

Mitochondrial Gene Expression and HS

cis-eQTLs were used as genetic tools for MR analysis, and 233 mitochondrial genes were found associated with HS (Supplementary Figure S2). *AMT* was identified as a protective factor for HS (OR=0.900, 95% CI:0.845–0.958, *P*<0.001, FDR=0.020). *GPD2* was also a protective factor for HS (OR=0.867, 95% CI:0.805–0.934, *P*<0.001, FDR=0.005). In contrast, *ATP5MC1* posed a risk for HS (OR=1.349, 95% CI:1.215–1.498, *P*<0.001, FDR<0.001). Similarly, *BAX* was a risk factor for HS (OR=1.294, 95% CI:1.152–1.452, *P*<0.001, FDR<0.001).

When considering the conditions of *P*<0.05 and I^2>50% in the heterogeneity analysis, it was indicated that 2 genes displayed significant heterogeneity: *LYPLAL1* (I^2=57%, Cochran's Q=71.312, *P*<0.001) and *MECR* (I^2=59%, Cochran's Q=9.849, *P*=0.043). The other gene loci did not show any significant heterogeneity.

The results of MR Egger regression and MR-PRESSO analysis indicated that three genes, namely *MPV17L2* (with P_{Egger}=0.010 and P_{PRESSO}=0.034), *GLYCTK* (with P_{Egger}=0.023 and P_{PRESSO}=0.049), and *NT5DC3* (with P_{Egger}=0.028 and P_{PRESSO}=0.039), had significant horizontal pleiotropy. The other 230 genes linked to HS did not show significant horizontal pleiotropy, suggesting that the MR results of this study were reliable (Supplementary Table S6).

Steiger filtering test results showed that the direction of mitochondrial gene expression in the HS dataset was "TRUE", suggesting mitochondrial genes related to the outcome aligned with what we expected (Supplementary Table S6).

Colocalization analysis of eQTLs for HS and mitochondrial genes showed that the PP.H4 value for *MRPS23* is 0.602>0.5, suggesting significant shared causal variants in this region (Supplementary Table S6).

Mitochondrial Protein and HS

cis-pQTLs were used as genetic tools for MR analysis, and 34 proteins (including 31 unique ones) were identified associated with HS (Figure 2). The IVW results indicated that 17 proteins acted as protective factors for HS, while 17 were identified as risk factors. RTN4IP1 is a protective factor for HS (OR= 0.354, 95% CI: 0.203–0.617, *P* < 0.001, FDR= 0.008); CASP9 is a protective factor for HS (OR= 0.459, 95% CI: 0.298–0.707, *P* < 0.001, FDR= 0.011); CAT is a risk factor for HS (OR= 1.462, 95% CI: 1.203–1.775, *P* < 0.001, FDR= 0.005); and FABP1 is also a risk factor for HS (OR= 1.367, 95% CI: 1.171–1.596, *P* < 0.001, FDR= 0.003).

For *P*<0.05 and I^2>50%, heterogeneity analysis revealed that two proteins showed heterogeneity in the IVW analysis: ACAA1 (I^2=36%, Cochran's Q=76.565, *P*= 0.007) and PDK1 (I^2=50%, Cochran's Q= 33.801, *P*= 0.009). The remaining ones did not show heterogeneity.

Horizontal pleiotropy analysis showed that there were two proteins with significant MR Egger regression intercepts (*P*<0.05), namely, FABP1 (*P*=0.026) and EFHD1 (*P*=0.043). The MR-PRESSO analysis indicated that there were two proteins with significant horizontal pleiotropy, specifically: PDK1 (*P*=0.005) and ACAA1 (*P*=0.006). The remaining 30 proteins associated with HS did not exhibit horizontal pleiotropy, suggesting that the MR results of this study were robust (Supplementary Table S7).

Steiger filtering test showed that the direction of mitochondrial proteins in the HS dataset is "TRUE", indicating that the causal relationship between mitochondrial proteins and the outcome aligned with what we expected (Supplementary Table S7).

							Heterogeneity		Horizontal pleiotropy		Steiger test		Colocalization
Cohort studies	Gene	Nsnp	OR(95%CI)	P value	FDR	I2(%)	P value	P value	MR-PRESSO P value	Correct_causal_direction	P value	PP.H4
Decode	ACAA1	50	0.843(0.724-0.981)	0.028	0.165	36	0.007	0.155	0.006	TRUE	0.00e+00	0.398
Decode	CAT	19	1.343(1.090-1.655)	0.006	0.061	29	0.118	0.244	0.122	TRUE	0.00e+00	0.020
Decode	COX4I2	6	0.445(0.268-0.740)	0.002	0.028	0	0.836	0.413	0.856	TRUE	1.04e-50	0.034
Decode	COX6A2	8	1.818(1.207-2.738)	0.004	0.051	0	0.948	0.979	0.937	TRUE	2.30e-69	0.040
Decode	CPOX	18	0.776(0.629-0.958)	0.018	0.125	0	0.719	0.313	0.665	TRUE	1.58e-262	0.018
Decode	CROT	66	0.905(0.833-0.983)	0.018	0.124	0	0.668	0.533	0.681	TRUE	0.00e+00	0.038
Decode	CRYZ	167	0.957(0.922-0.993)	0.020	0.135	0	0.976	0.479	0.973	TRUE	-	0.021
Decode	ECI2	76	1.113(1.034-1.198)	0.004	0.049	0	0.810	0.881	0.832	TRUE	0.00e+00	0.024
Decode	HIBCH	67	1.151(1.046-1.266)	0.004	0.049	0	0.694	0.894	0.734	TRUE	0.00e+00	0.045
Decode	HTATIP2	171	1.110(1.051-1.172)	<0.001	0.005	0	0.483	0.796	0.496	TRUE	0.00e+00	0.030
Decode	IVD	13	0.755(0.597-0.955)	0.019	0.129	0	0.844	0.195	0.862	TRUE	2.51e-179	0.023
Decode	MMAB	66	0.827(0.750-0.912)	<0.001	0.005	19	0.094	0.432	0.107	TRUE	0.00e+00	0.045
Decode	NUDT9	7	0.713(0.516-0.985)	0.040	0.206	0	0.763	0.835	0.782	TRUE	1.25e-119	0.036
Decode	PARK7	10	1.398(1.066-1.832)	0.015	0.115	0	0.618	0.339	0.593	TRUE	4.14e-162	0.036
Decode	PDK1	18	0.652(0.504-0.844)	0.001	0.022	50	0.009	0.462	0.005	TRUE	0.00e+00	0.046
Decode	RPIA	19	1.330(1.016-1.740)	0.038	0.199	36	0.058	0.134	0.086	TRUE	2.46e-271	0.020
Decode	RTN4IP1	5	0.354(0.203-0.617)	<0.001	0.008	0	0.546	0.401	0.640	TRUE	7.07e-41	0.039
UKB-ppp	ACADM	9	0.730(0.538-0.991)	0.043	0.214	0	0.513	0.581	0.567	TRUE	7.64e-141	0.025
UKB-ppp	ATP5IF1	7	0.606(0.373-0.983)	0.043	0.212	33	0.180	0.559	0.302	TRUE	1.18e-81	0.032
UKB-ppp	C2orf69	7	0.539(0.340-0.856)	0.009	0.082	0	0.673	0.948	0.731	TRUE	3.47e-81	0.068
UKB-ppp	CA5A	92	1.081(1.015-1.151)	0.015	0.111	0	0.747	0.104	0.759	TRUE	0.00e+00	0.025
UKB-ppp	CASP9	5	0.459(0.298-0.707)	<0.001	0.011	0	0.704	0.386	0.785	TRUE	1.43e-59	0.102
UKB-ppp	CAT	22	1.462(1.203-1.775)	<0.001	0.005	20	0.200	0.378	0.204	TRUE	0.00e+00	0.020
UKB-ppp	ECHDC3	103	1.085(1.023-1.150)	0.007	0.067	0	0.825	0.624	0.841	TRUE	0.00e+00	0.032
UKB-ppp	ECI2	32	1.176(1.033-1.338)	0.014	0.111	0	0.806	0.600	0.819	TRUE	0.00e+00	0.026
UKB-ppp	EFHD1	33	1.153(1.001-1.328)	0.048	0.227	23	0.125	0.043	0.145	TRUE	0.00e+00	0.026
UKB-ppp	FABP1	31	1.367(1.171-1.596)	<0.001	0.003	10	0.316	0.026	0.351	TRUE	0.00e+00	0.019
UKB-ppp	FHIT	10	1.515(1.057-2.171)	0.024	0.149	9	0.358	0.281	0.395	TRUE	2.21e-107	0.022
UKB-ppp	GLRX5	15	1.347(1.061-1.709)	0.014	0.111	0	1.000	0.817	1.000	TRUE	1.96e-224	0.043
UKB-ppp	GRHPR	41	0.826(0.725-0.941)	0.004	0.049	4	0.406	0.293	0.470	TRUE	0.00e+00	0.020
UKB-ppp	MTHFD2	6	1.995(1.120-3.552)	0.019	0.129	15	0.320	0.620	0.406	TRUE	5.49e-57	0.094
UKB-ppp	RIDA	22	0.591(0.494-0.709)	<0.001	0.000	27	0.119	0.186	0.161	TRUE	0.00e+00	0.278
UKB-ppp	RTN4IP1	12	0.566(0.422-0.760)	<0.001	0.005	0	0.576	0.983	0.591	TRUE	8.94e-150	0.142
UKB-ppp	TDRKH	52	1.117(1.001-1.247)	0.049	0.229	0	0.963	0.954	0.972	TRUE	0.00e+00	0.018

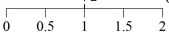

Figure 2 Associations of genetically predicted mitochondrial gene encoded protein with HS in Mendelian randomization analysis.
Abbreviations: OR, odds ratio; FDR, false discovery rate; PPH4, posterior probability of H4.

Colocalization analysis of pQTLs for HS and mitochondrial genes indicated that there was no evidence of colocalization between the mitochondrial gene pQTLs and HS (Supplementary Table S7).

Integrating Evidence from Multi-Omics Levels

After integrating multiple omics evidence, this study identified two genes associated with HS that have strong multi-omics evidence: *HTATIP2* and *PDK1*. The FDR values for these two genes in methylation, gene expression, and protein levels were all below 0.05. Moreover, cg01397325 (*HTATIP2*) methylation was linked to a lower risk of HS (OR= 0.925, *P*<0.001), and cg24426391 (*HTATIP2*) methylation was also linked to a lower risk of HS (OR= 0.961, *P*=0.002). The gene expression (OR=1.171, *P*<0.001) and protein abundance (OR=1.110, *P*<0.001) of *HTATIP2* were both associated with a higher risk of HS. Methylation of *PDK1*'s CpG site cg04033559 (OR=0.937, *P*<0.001) was linked to a lower risk of HS, whereas methylation of *PDK1*'s CpG sites cg10165864 (OR=1.298, *P*<0.001) and cg17679246 (OR=1.188, *P*<0.001) was linked to a higher HS risk. The gene expression (OR=0.759, *P*<0.001) and protein abundance (OR=0.625, *P*<0.001) of *PDK1* were both negatively correlated with the risk of HS (Figure 3 and Table 2).

Sixteen genes were identified tier 2 genes associated with HS, including *CARS2, CASP9, COMT, DGUOK, MMAB, MRPL21, MSRA, NDUFS2, NSUN2, NT5DC2, NT5DC3, PRDX5, RDH13, RIDA, SND1*, and *TRAP1*. The FDR for all these genes was less than 0.05. The following CpG sites were associated with risk factors for HS: cg11716795 of *MRPL21* (OR=1.097, *P*< 0.001), cg17964305 of *MSRA* (OR=1.463, *P*=0.001), cg23400122 of *MSRA* (OR=1.238, P<0.001), cg26077133 of *MSRA* (OR=1.045, *P*<0.001), cg26420013 of *NSUN2* (OR=1.172, *P*=0.002), cg22710716 of *NT5DC2* (OR=1.051, *P*=0.002), cg21863207 of *NT5DC3* (OR=1.102, *P*=0.001), cg01708924 of *PRDX5* (OR=1.371, *P*=0.001), cg02592727 of *RDH13* (OR=1.096, *P*=0.004), cg07598936 of *RDH13* (OR=1.138, *P*<0.001), cg08278892 of *RDH13* (OR=1.146, *P*=0.003), cg00893242 of *SND1* (OR=1.121, *P*<0.001), cg06714981 of *SND1* (OR=1.055, *P*=0.002), and cg11539674 of *SND1* (OR=1.093, *P*<0.001). The gene expression of *CASP9* (OR=0.849, *P*<0.001), *COMT* (OR=0.837, *P*<0.002), *MMAB* (OR=0.711, *P*<0.001), *MRPL21* (OR=0.903, *P*<0.001), *NDUFS2* (OR=0.685, *P*<0.001), *NSUN2* (OR=0.930, *P*<0.002), *NT5DC3* (OR=0.903, *P*<0.001), *RDH13* (OR=0.907, *P*<0.001), *RIDA*

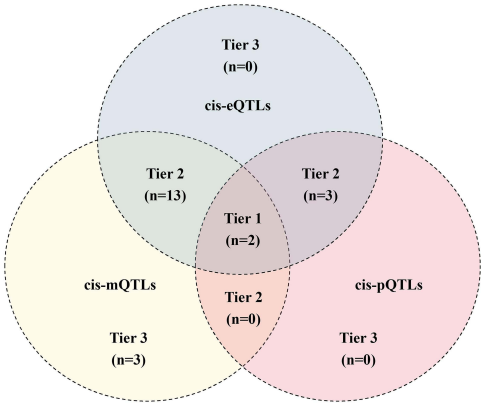

Figure 3 Grading results for HS candidate genes.
Abbreviations: HS, hypertrophic scars; QTL, quantitative trait loci.

(OR=0.559, *P*<0.001), *SND1* (OR=0.679, *P*<0.001), and *TRAP1* (OR=0.890, *P*<0.001) were protective factors for HS. The protein levels of *CASP9* (OR=0.459, *P*<0.001), *MMAB* (OR=0.827, P<0.001), and *RIDA* (OR=0.591, P<0.001) also served as protective factors for HS (Figure 3 and Table 3).

IMMT, MRPL23, and *USP30* genes were identified as tier 3 genes associated with HS. Among the tier 3 genes, the methylation of cg07610327 in *IMMT* was a risk factor for HS (OR=1.191, *P*<0.001), while cg06498964 (OR=0.829, *P*<0.001) and cg07578618 (OR=0.820, *P*<0.001) in the *MRPL23* were protective factors for HS. Methylation of cg03124318 (OR=0.828, *P*<0.001) and cg12535380 (OR=0.863, *P*<0.001) in *USP30* was also a protective factor for HS (Figure 3 and Table 4).

Tissue-Specific Verification

The levels of HTATIP2 expression in normal skin (NS) and hypertrophic scar tissue (HS) were assessed by qRT-PCR, Western blot analysis, and immunofluorescence techniques. Notably, both mRNA and protein concentrations of HTATIP2 exhibited a significant elevation in the HS cohort in comparison to the NS group (Figure 4A and B). Furthermore, HSF and NSF were isolated from HS and NS tissues, respectively. Subsequently, cell immunofluorescence was conducted to measure the intracellular expression levels of HTATIP2. The results indicated that HTATIP2 intensity was substantially greater in the HSF group relative to the NSF group, as depicted in Figure 4C.

A schematic summary of the multi-omics integration process was in Figure 5.

Table 2 Genetically Predicted Methylation, Expression, and Protein of Tier 1 Candidate Gene with HS in Mendelian Randomization

Gene	mQTLs			eQTLs		pQTLs	
	Probe ID	OR (95% CI)	FDR	OR (95% CI)	FDR	OR (95% CI)	FDR
HTATIP2	cg01397325	0.925 (0.884–0.967)	0.015	1.171 (1.109–1.237)	<0.001	1.110 (1.051–1.172)	0.005
	cg24426391	0.961 (0.937–0.985)	0.030	1.171 (1.109–1.237)	<0.001	1.110 (1.051–1.172)	0.005
PDK1	cg04033559	0.937 (0.905–0.970)	0.008	0.759 (0.682–0.845)	<0.001	0.652 (0.504–0.844)	0.022
	cg10165864	1.298 (1.159–1.454)	<0.001	0.759 (0.682–0.845)	<0.001	0.652 (0.504–0.844)	0.022
	cg17679246	1.188 (1.099–1.284)	<0.001	0.759 (0.682–0.845)	<0.001	0.652 (0.504–0.844)	0.022

Abbreviations: mQTL, methylation quantitative trait loci; eQTL, expression quantitative trait loci; pQTL, protein quantitative trait loci; OR, odds ratio; CI, confidence interval; FDR, false discovery rate.

https://doi.org/10.2147/JIR.S567534

Table 3 Genetically Predicted Methylation, Expression, and Protein of Tier 2 Candidate Gene with HS in Mendelian Randomization

Gene	mQTLs			eQTLs		pQTLs	
	Probe ID	OR (95% CI)	FDR	OR (95% CI)	FDR	OR (95% CI)	FDR
CARS2	cg15747390	0.930 (0.890–0.973)	0.024	1.197 (1.109–1.291)	<0.001		
	cg20124610	0.818 (0.729–0.919)	0.015	1.197 (1.109–1.291)	<0.001		
CASP9				0.849 (0.770–0.936)	0.021	0.459 (0.298–0.707)	0.011
COMT	cg10122187	0.830(0.747–0.922)	0.013	0.837 (0.749–0.936)	0.029		
DGUOK	cg03063511	0.874(0.804–0.950)	0.025	1.288 (1.088–1.525)	0.043		
MMAB				0.711 (0.589–0.857)	0.010	0.827 (0.750–0.912)	0.005
MRPL21	cg11716795	1.097(1.046–1.150)	0.005	0.903 (0.872–0.936)	<0.001		
MSRA	cg02319733	0.924 (0.900–0.948)	<0.001	1.131 (1.088–1.176)	<0.001		
	cg05753693	0.883 (0.828–0.942)	0.005	1.131 (1.088–1.176)	<0.001		
	cg06620390	0.853 (0.810–0.898)	<0.001	1.131 (1.088–1.176)	<0.001		
	cg08841257	0.914 (0.887–0.942)	<0.001	1.131 (1.088–1.176)	<0.001		
	cg11548083	0.929 (0.904–0.954)	<0.001	1.131 (1.088–1.176)	<0.001		
	cg12345456	0.870 (0.800–0.945)	0.020	1.131 (1.088–1.176)	<0.001		
	cg12940923	0.937 (0.918–0.956)	<0.001	1.131 (1.088–1.176)	<0.001		
	cg14257676	0.923 (0.893–0.954)	<0.001	1.131 (1.088–1.176)	<0.001		
	cg16038868	0.931 (0.905–0.957)	<0.001	1.131 (1.088–1.176)	<0.001		
	cg17964305	1.463 (1.166–1.835)	0.020	1.131 (1.088–1.176)	<0.001		
	cg21915799	0.924 (0.897–0.951)	<0.001	1.131 (1.088–1.176)	<0.001		
	cg23400122	1.238 (1.106–1.386)	0.007	1.131 (1.088–1.176)	<0.001		
	cg26077133	1.045 (1.029–1.062)	<0.001	1.131 (1.088–1.176)	<0.001		
NDUFS2	cg04436964	0.912 (0.872–0.953)	0.002	0.685 (0.574–0.817)	0.001		
NSUN2	cg26420013	1.172 (1.062–1.293)	0.026	0.930 (0.888–0.975)	0.034		
NT5DC2	cg05564831	0.928 (0.887–0.971)	0.023	1.232 (1.151–1.319)	<0.001		
	cg17372223	0.937 (0.902–0.973)	0.015	1.232 (1.151–1.319)	<0.001		
	cg22710716	1.051 (1.018–1.084)	0.031	1.232 (1.151–1.319)	<0.001		
NT5DC3	cg21863207	1.102 (1.039–1.169)	0.023	0.903 (0.864–0.944)	<0.001		
PRDX5	cg01708924	1.371 (1.132–1.660)	0.023	1.133 (1.080–1.189)	<0.001		
RDH13	cg02592727	1.096 (1.030–1.166)	0.048	0.907 (0.876–0.939)	<0.001		
	cg07598936	1.138 (1.060–1.222)	0.010	0.907 (0.876–0.939)	<0.001		
	cg08278892	1.146 (1.048–1.252)	0.039	0.907 (0.876–0.939)	<0.001		
RIDA				0.559 (0.476–0.657)	<0.001	0.591 (0.494–0.709)	<0.001
SND1	cg00893242	1.121 (1.048–1.199)	0.019	0.679 (0.556–0.830)	0.005		
	cg06714981	1.055 (1.020–1.091)	0.028	0.679 (0.556–0.830)	0.005		
	cg07304760	0.923 (0.900–0.946)	<0.001	0.679 (0.556–0.830)	0.005		
	cg11539674	1.093 (1.059–1.128)	<0.001	0.679 (0.556–0.830)	0.005		
TRAP1	cg24062157	0.937 (0.898–0.979)	0.045	0.890 (0.833–0.952)	0.015		

Abbreviations: mQTL, methylation quantitative trait loci; eQTL, expression quantitative trait loci; pQTL, protein quantitative trait loci; OR, odds ratio; CI, confidence interval; FDR, false discovery rate.

Discussion

This study focused on the causal relationship between mitochondrial-related genes and HS. At present, there is a consensus on the mechanisms of HS formation, which relate to the release of different growth factors, persistent inflammation, overproduction of fibroblasts (with less apoptosis and more proliferation), and excessive deposition of collagen. Additionally, the formation of new blood vessels also plays a key role in HS development.[13,14] There are five main signaling pathways involved in scar formation: Wnt/β-catenin, TGF-β, Notch, Sonic Hedgehog, and Ras/MEK/ERK signaling pathways.[32] Previous studies showed that mitochondrial function was closely linked to cell growth, apoptosis, and oxidative stress.[20,21] Consequently, alterations in mitochondrial genes could affect the chances of developing HS. These links lay the groundwork for this study.

Table 4 Genetically Predicted Methylation, Expression, and Protein of Tier 3 Candidate Gene with HS in Mendelian Randomization

Gene	mQTLs			
	Probe ID	OR (95% CI)	FDR	PPH4
IMMT	cg07610327	1.191(1.089–1.303)	0.005	0.595
MRPL23	cg06498964	0.829(0.747–0.921)	0.012	0.861
	cg07578618	0.820(0.756–0.889)	<0.001	0.712
USP30	cg03124318	0.828(0.761–0.901)	<0.001	0.549
	cg12535380	0.863(0.813–0.915)	<0.001	0.743

Abbreviations: mQTL, methylation quantitative trait loci; OR, odds ratio; CI, confidence interval; FDR, false discovery rate; PPH4, posterior probability of H4.

Previous studies on mitochondria and HS mainly focused on molecules sourced from research on tumors and myocardial infarction, such as those affecting tumor proliferation, apoptosis, and ROS generation, to check their effects on scars and scar fibroblasts.[33] There has not been much research identifying key genes through large-scale, high-throughput data screening, and even when it's done, it typically focused on the RNA expression of differentially expressed genes.[34,35] Such research paid less attention to a comprehensive look at gene transcription, translation, and regulation and lacked a solid scientific basis for multi-omics screening of target molecules. This study used data from several cohorts related to mitochondrial genes, screening HS-related genes by looking at three aspects: DNA methylation, RNA expression, and protein abundance. After a series of validity checks, the reliability of the screening results was confirmed, which meant it has broader applications for finding potential candidate genes for HS.

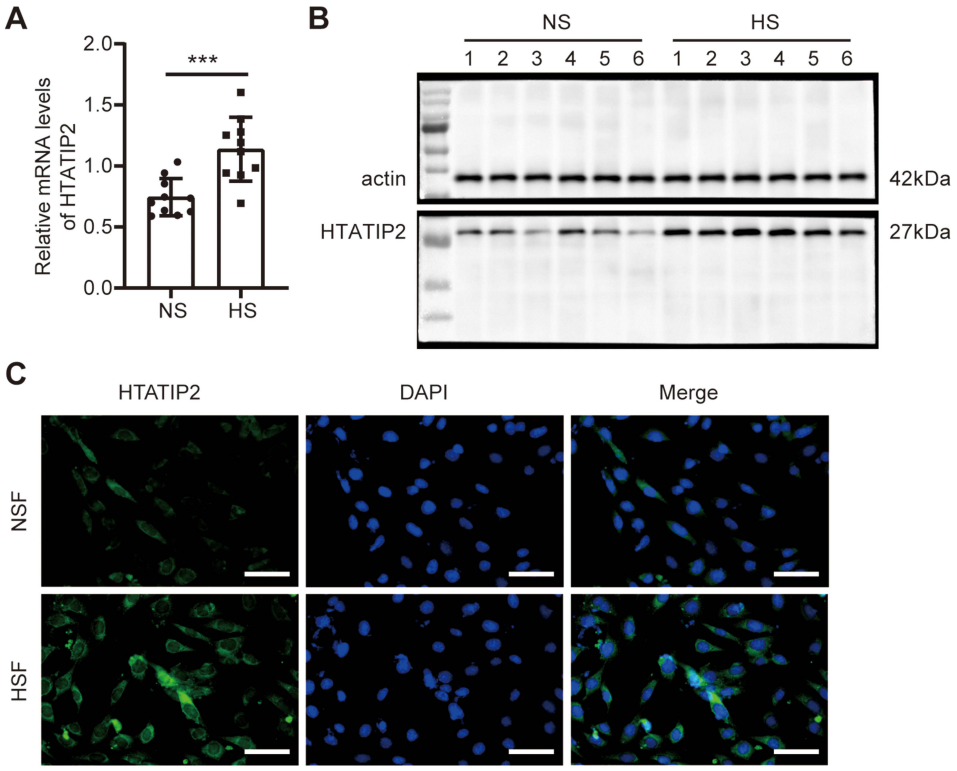

Figure 4 The expression of HTATIP2 in skin tissues of patients with HS. (**A**) The mRNA levels of HTATIP2 in normal skin and hypertrophic scar tissues were detected by qRT-PCR. (**B**) The protein levels of HTATIP2 in normal skin and hypertrophic scar tissues were detected by Western blot. (**C**) The HTATIP2 expression NSF and HSF was detected by cell immunofluorescence. Scale bar: 50μm. ***$p < 0.001$ using unpaired two-tailed Student's *t*-test. Data are presented as mean ± SD.
Abbreviations: NS, Normal Skin; HS, Hypertrophic Scar; NSF, Normal Skin Fibroblast; HSF, Hypertrophic Scar:Fibroblast.

https://doi.org/10.2147/JIR.S567534

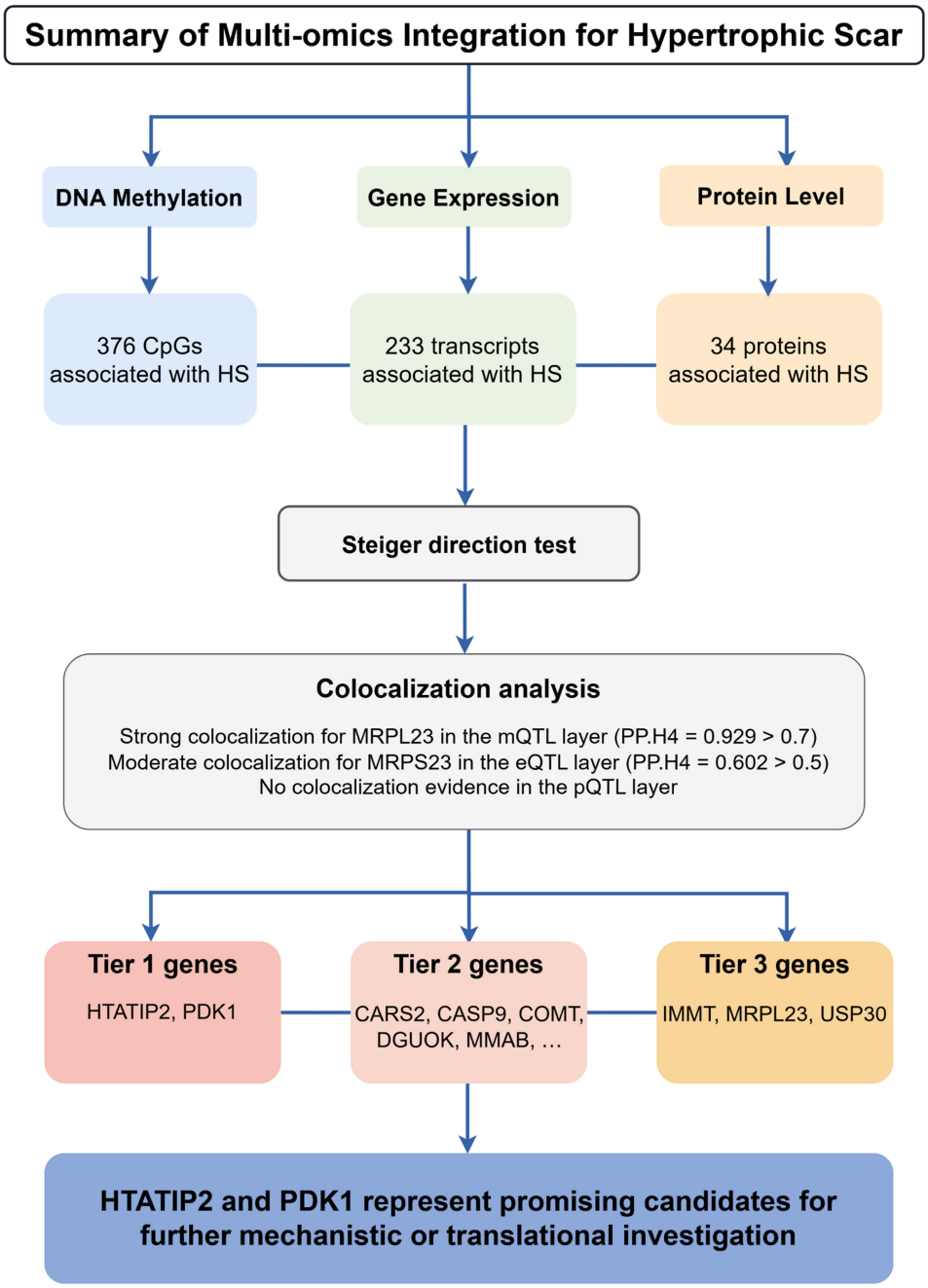

Figure 5 A schematic diagram of the multi-omics integration process. Figure created by Figdraw.

HTATIP2, also known as *TIP30* or *CC3*, is a redox enzyme essential for tumor suppression, primarily involved in nuclear transport and the regulation of angiogenesis, and playing a role in regulating programmed cell death.[36] Previous studies found that gene methylation negatively correlates with RNA and protein expression. Our multi-omics results showed that both DNA methylation sites of *HTATIP2* were negatively correlated with HS, while *HTATIP2* gene expression and protein levels were positively correlated with HS formation and development. Some researchers found that methylation of *HTATIP2* led to downregulation of gene expression in uterine leiomyoma, which aligned with our multi-omics results.[37] Therefore, the relationship between *HTATIP2* methylation and RNA expression/protein abundance in relation to HS matched what previous studies have reported.

However, there were few reports on the relationship between HTATIP2 and HS. Previous studies revealed that the formation of uncontrolled blood vessel growth could lead to persistent inflammation and ultimately result in HS.[38] Additionally, blocking the growth of new blood vessels in endothelial cells effectively reduced HS formation.[39] Research has shown that higher levels of HTATIP2 reduced the ability to form new blood vessels in patients with chronic limb-threatening ischemia (CLTI), while downregulating its expression enhanced the factors in macrophages isolated from CLTI patients that regulate blood vessel growth, such as Neuropilin-1 and Angiopoietin-1, promoting blood vessel growth (endothelial tube formation assays) and arterial formation (smooth muscle proliferation).[40] Studies on liver cancer also confirmed that HTATIP2 promoted cell death and inhibited blood vessel growth.[41,42]

The formation of HS is closely related to increased proliferation of fibroblasts and reduced apoptosis. Apoptosis is a physiological process of cell self-destruction carried out in a programmed way.[43] Previous literature has reported that increasing the proliferation capacity of fibroblasts and inhibiting their apoptosis could promote scar formation.[43–45] In lab experiments, HTATIP2 was found to make fibroblasts more sensitive to apoptosis.[36] This goes against our findings that the gene expression and protein levels of HTATIP2 were risk factors for HS.

One of the characteristics of HS is the excessive proliferation of fibroblasts and the excessive deposition of extracellular matrix (ECM).[46,47] In the dysregulated wound healing process, specialized myofibroblasts proliferate excessively, leading to abnormal accumulation of ECM.[48] The Wnt pathway plays an important role in the pathological mechanisms of keloids and HS.[49] Some research indicated that Interferon-α2b could inhibit the proliferation and migration of HS fibroblasts by suppressing the Wnt pathway.[50] In interaction models of fibroblasts and endothelial cells, some researchers found that in both in vitro and in vivo models, the Wnt pathway could regulate the cellular activities of fibroblasts.[51] In a review on chronic kidney disease, some scholars also mentioned that the Wnt pathway could activate myofibroblasts, leading to excessive ECM deposition.[52] An integrative analysis of the DNA methylome and transcriptome in uterine leiomyoma showed that *HTATIP2* was related to the ECM deposition and the dysregulation of the Wnt/β-catenin pathway.[37] These studies indicated that the Wnt pathway could promote excessive deposition of ECM by activating myofibroblasts, which could lead to HS. And previous studies also revealed that *HTATIP2* could interfere with the Wnt pathway, leading to pathway dysregulation, which contradicted our findings that *HTATIP2* gene expression and protein levels were risk factors for HS.

The TGF-β pathway and Notch pathway play important roles in the formation of HS. The TGF-β pathway is the most well-known signaling pathway regulating the biological behavior of fibroblasts and collagen formation. Continuous activation of this pathway leads to excessive activation of fibroblasts, ultimately causing excessive collagen deposition and the formation of HS.[53] During the wound healing process, timely intervention in TGF-β effectively reduces the formation of HS.[54] Blocking Notch signaling in macrophages could reduce inflammation in the wound tissue through intercellular signaling and inhibit collagen synthesis by fibroblasts.[55] Moreover, the Notch signaling pathway promotes HS formation by regulating the subtypes of epidermal cells.[56] In pancreatic cancer research, researchers found that inhibiting HTATIP2 enhanced miR-10b's role in promoting TGF-β, enhancing EGFR signaling, facilitating EGF-TGF-β cross-talk and promoting the expression of EMT-promoting genes.[57] In multiple sclerosis (MS) research, *HTATIP2* acts as a pro-apoptotic factor, inhibiting nuclear transport and, consequently, Notch1-mediated oligodendrocyte differentiation and remyelination.[58] These research results suggested that *HTATIP2* might inhibit HS formation through the TGF-β pathway and Notch pathway, which contradicted our findings that *HTATIP2* gene expression and protein abundance were positively correlated with HS.

Previous studies have shown that HTATIP2 may have a negative effect on HS, which is at odds with our results. The reasons for this are as follows. First, the diseases targeted by different studies varied, and most studies focused on tumors. Tumor microenvironments differ from those of wounds or scars,[59] which means the same gene might work differently in various environments, and might even do the opposite. Second, previous studies mainly focused on the regulatory level of a single gene, while our research integrated multi-omics results of the methylation, gene expression and protein levels in mitochondrial related genes. So earlier studies might not give the full picture. Our multi-omics findings suggested that the *HTATIP2* gene could play a role in how HS develops, which needs more research in the future.

Pyruvate dehydrogenase (PDH) is a mitochondrial multienzyme complex that catalyzes the oxidative decarboxylation of pyruvate and is one of the key enzymes responsible for regulating carbohydrate fuel homeostasis in mammals. Its

activity is regulated by a cycle of phosphorylation and dephosphorylation. PDK1 (Pyruvate Dehydrogenase Kinase 1) catalyzes the phosphorylation of pyruvate dehydrogenase, leading to its inactivation, playing a key role in regulating glucose and fatty acid metabolism and overall metabolic homeostasis.[58,60] It downregulates aerobic respiration and inhibits the conversion of pyruvate to acetyl-CoA by regulating the metabolic flux of tricarboxylic acid cycle metabolites, playing an important role in the cellular response to hypoxia, which is vital for cell proliferation in low-oxygen conditions, protecting cells from apoptosis caused by hypoxia and oxidative stress.[61] Research shows that low-oxygen conditions boost glycolysis while weakening mitochondrial function, resulting in increased proliferation and migration in scar fibroblasts, increased collagen synthesis, and inhibition of apoptosis. So, the molecular changes in glucose metabolism and mitochondrial function due to hypoxia could be potential targets for treating HS and keloids.[35]

The direct clinical relationship between PDK1 and scars has not been reported. A search on the cell biological behaviors related to scars found that in cases of pulmonary hypertension, the DNMT1-HIF-1α-PDK pathway could reduce fibroblast proliferation and collagen production.[62] In terms of cellular senescence, some researchers found that inhibiting PDK1 could alleviate cellular senescence and skin atrophy, which specifically promotes fibroblast proliferation and collagen deposition when PDK1 was inhibited.[63] Interestingly, some researchers noted that in the fibrosis of various diseases, inhibiting PDK1 led to fibroblast apoptosis and reduced collagen production.[64] Previous studies suggested that *PDK1* could both promote and inhibit the development of HS. This might be due to different methylation sites of *PDK1*, which still needs to be tested experimentally.

The repair process of wounds constantly requires the involvement of inflammatory responses.[65] HS are consequences of a dysregulated wound healing process, which involves inflammatory responses in their occurrence and development.[13] T cells, as key cells in the inflammatory response, through their production, development, and differentiation, play a crucial role in the direction of the inflammatory response and the emergence of different clinical outcomes. T cells are linked to scar formation, and those with different differentiation have varying effects on HS. IL-10-producing T lymphocytes regulate inflammatory cell cytokine expression to promote hyaluronan-rich ECM deposition and attenuate fibrosis. Promoting IL-10-producing lymphocytes in wounds may be a therapeutic target to promote regenerative or scarless wound healing.[66] Previous studies showed that PDK1 was crucial for T cell development, differentiation, and homeostasis, and "knockout of PDK1 in lymphocytes hindered T cell development in the thymus and exhibited a substantial influence on immune cell homeostasis in the spleen and lymph nodes".[67] Lack of PDK1 could disrupt T cell-mediated inflammatory responses, leading to inflammatory skin diseases.[68] Research on scarring pathways found that *PDK1* is linked to the Wnt/β-Catenin, Notch, and Ras/ERK/MEK pathways.[69–71] It's important to note that *PDK1* regulates Notch-induced T cell development.[72] PDK1 also helps promote the differentiation of T follicular helper cells via the PI3K/AKT pathway.[73] In summary, this study revealed that *PDK1* likely regulated T cell development through the Notch and PI3K/AKT pathways, shaping the inflammatory response and ultimately impacting HS formation.

In the search for scar-related studies on tier 2 and tier 3 genes identified through multi-omics integration, three previously reported genes associated with HS formation were noted: COMT, SND1, and TRAP1. COMT (Catechol-O-methyltransferase) catalyzes the transfer of a methyl group from S-adenosylmethionine to catecholamines, including the neurotransmitters dopamine, epinephrine, and norepinephrine. This O-methylation is one of the primary degradation pathways for catecholamine neurotransmitters.[74] Previous studies have reported that catecholamines are related to scar formation. For example, dopamine could regulate inflammatory responses and scar formation, which is why many wound healing materials include dopamine to help reduce scarring.[75,76] A prospective cohort study found that a specific variant of the COMT gene (AA rs4680 genotype) may protect against scarring and itching after burns.[77] SND1 is known to be an oncogene in several tumors, highly expressed in burned skin tissue, and could promote the formation of HS through the ERK/JNK signaling pathway, which makes it a risk factor for HS formation.[78] TRAP1, as a molecular chaperone of Smad4, could bring Smad4 into the vicinity of the TGF-β receptor complex and mediate downstream signaling, regulating the formation and contraction of HS.[79] These three genes are relevant to our findings and deserve further investigation. However, there are not many reports on the other 18 genes linked to HS. Nevertheless, these genes, although not previously reported, still hold value for research and could help fill gaps in understanding the pathogenesis of HS.

The inclusion of multiple validation steps-heterogeneity testing, pleiotropy correction, and colocalization enhances robustness in this study. The PP.H4>0.7 threshold has been widely used in recent multi-omics integration and causal inference studies to see if two traits are driven by the same causal variant.[80,81] These studies all back up using PP.H4>0.7 as a well-accepted empirical threshold for colocalization analysis today. We also recognize that the interpretation of PP.H4 should be considered alongside the specific research context and biological plausibility, instead of just relying on one threshold. Therefore, in this study, in addition to sharing the PP.H4 results, we also incorporated the Steiger direction test (to check if the causal direction is consistent), tests for heterogeneity (Cochran's Q and I^2), and MR-PRESSO to detect pleiotropy. This helps us assess the robustness of the analysis results from different angles. These tests can be seen as sensitivity analyses for our study, helping to reduce the instability of results caused by different model assumptions or biases from single instrumental variables.

One of the primary limitations of this study is the lack of wet lab validation to corroborate the bioinformatics findings. Our analysis mainly shows a potential causal link between genetic regulation at the systemic level and the risk of hypertrophic scars, but we still need to validate the specific mechanisms in future studies that look into the functional research on local tissues. Additionally, the study population is predominantly of European descent, which may limit the generalizability of the findings to other ethnic groups. This demographic constraint necessitates further research involving diverse populations to ensure broader applicability. These limitations highlight the need for comprehensive follow-up studies to validate and extend our findings.

This study found 21 mitochondrial genes that could be potential targets, with *HTATIP2* and *PDK1* being the most promising for clinical use. This research lays a solid foundation for further exploration into how HS forms at the molecular level and gives us some hopeful targets for HS management.

Data Sharing Statement

Data supporting the findings of this study are available from the corresponding author upon reasonable request.

Ethics Approval and Consent to Participate

This study was conducted in accordance with the Declaration of Helsinki and approved by the Ethics Committee of Fujian Medical University Union Hospital (2025KY428). Written informed consent was obtained from all the participants.

Acknowledgment

We acknowledge the editors and reviewers for their helpful comments on this paper.

Author Contributions

Conceptualization: Teng Gong, Zhaohong Chen, Minjuan Wu.
Data curation: Teng Gong, Jiansheng Zheng.
Formal analysis: Teng Gong, Minjuan Wu.
Investigation: Teng Gong, Minjuan Wu.
Methodology: Teng Gong, Jiansheng Zheng.
Project administration: Minjuan Wu, Zhaohong Chen.
Supervision: Teng Gong, Zhaohong Chen.
Funding acquisition: Teng Gong.
Writing – original draft: Teng Gong, Jiansheng Zheng, Zhaohong Chen, Minjuan Wu.
Writing – review & editing: Teng Gong, Jiansheng Zheng, Zhaohong Chen, Minjuan Wu.

Teng Gong, Minjuan Wu, Jiansheng Zheng are co-first authors. All authors took part in drafting, revising or critically reviewing the article; gave final approval of the version to be published; have agreed on the journal to which the article has been submitted; and agree to be accountable for all aspects of the work.

Funding

This study was supported by the National Natural Science Foundation of China (32071186), Fujian Provincial Natural Science Foundation of China (2022J01243), Joint Funds for the innovation of Science and Technology, Fujian Province (2023Y9213), High-level Hospital and Clinical Specialty Discipline Construction Program for Fujian Medical Development, China ([2021]76), and Fujian Provincial Key Laboratory of Burn and Trauma, China.

Disclosure

The authors declare that they have no competing interests.

References

1. Wang J, Zhao M, Zhang H, et al. KLF4 alleviates hypertrophic scar fibrosis by directly activating BMP4 transcription. *Int J Biol Sci*. 2022;18(8):3324–3336. doi:10.7150/ijbs.71167
2. Leszczynski R, da Silva CA, Pinto A, Kuczynski U, da Silva EM. Laser therapy for treating hypertrophic and keloid scars. *Cochrane Database Syst Rev*. 2022;9(9):CD011642. doi:10.1002/14651858.CD011642.pub2
3. Yin J, Zhang S, Yang C, et al. Mechanotransduction in skin wound healing and scar formation: potential therapeutic targets for controlling hypertrophic scarring. *Front Immunol*. 2022;13:1028410. doi:10.3389/fimmu.2022.1028410
4. Mony MP, Harmon KA, Hess R, Dorafshar AH, Shafikhani SH. An updated review of hypertrophic scarring. *Cells*. 2023;12(5):678. doi:10.3390/cells12050678
5. Frech FS, Hernandez L, Urbonas R, Zaken GA, Dreyfuss I, Nouri K. Hypertrophic scars and keloids: advances in treatment and review of established therapies. *Am J Clin Dermatol*. 2023;24(2):225–245. doi:10.1007/s40257-022-00744-6
6. Yuan B, Upton Z, Leavesley D, Fan C, Wang XQ. Vascular and collagen target: a rational approach to hypertrophic scar management. *Adv Wound Care*. 2023;12(1):38–55. doi:10.1089/wound.2020.1348
7. Cui HS, Joo SY, Lee SY, Cho YS, Kim DH, Seo CH. Effect of hypertrophic scar fibroblast-derived exosomes on keratinocytes of normal human skin. *Int J Mol Sci*. 2023;24(7):6132. doi:10.3390/ijms24076132
8. Fernández-Guarino M, Bacci S, Pérez González LA, Bermejo-Martínez M, Cecilia-Matilla A, Hernández-Bule ML. The role of physical therapies in wound healing and assisted scarring. *Int J Mol Sci*. 2023;24(8):7487. doi:10.3390/ijms24087487
9. Lin TR, Chou FH, Wang HH, Wang RH. Effects of scar massage on burn scars: a systematic review and meta-analysis. *J Clin Nurs*. 2023;32(13–14):3144–3154. doi:10.1111/jocn.16420
10. He J, Fang B, Shan S, et al. Mechanical stretch promotes hypertrophic scar formation through mechanically activated cation channel Piezo1. *Cell Death Dis*. 2021;12(3):226. doi:10.1038/s41419-021-03481-6
11. Ogawa R. The most current algorithms for the treatment and prevention of hypertrophic scars and keloids: a 2020 update of the algorithms published 10 years ago. *Plast Reconstr Surg*. 2022;149(1):79e–94e. doi:10.1097/PRS.0000000000008667
12. Monzel AS, Enríquez JA, Picard M. Multifaceted mitochondria: moving mitochondrial science beyond function and dysfunction. *Nat Metab*. 2023;5(4):546–562. doi:10.1038/s42255-023-00783-1
13. Wang ZC, Zhao WY, Cao Y, et al. The roles of inflammation in keloid and hypertrophic scars. *Front Immunol*. 2020;11:603187. doi:10.3389/fimmu.2020.603187
14. Li J, Yin Y, Zhang E, Gui M, Chen L, Li J. Peptide deregulated in hypertrophic scar-1 alleviates hypertrophic scar fibrosis by targeting focal adhesion kinase and pyruvate kinase M2 and remodeling the metabolic landscape. *Int J Biol Macromol*. 2023;235:123809. doi:10.1016/j.ijbiomac.2023.123809
15. Liu BH, Chen L, Li SR, Wang ZX, Cheng WG. Smac/DIABLO regulates the apoptosis of hypertrophic scar fibroblasts. *Int J Mol Med*. 2013;32(3):615–622. doi:10.3892/ijmm.2013.1442
16. Xiao Y, Xu D, Song H, et al. Cuprous oxide nanoparticles reduces hypertrophic scarring by inducing fibroblast apoptosis. *Int J Nanomed*. 2019;14:5989–6000. doi:10.2147/IJN.S196794
17. Hsieh SC, Wu CC, Hsu SL, Yen JH. Molecular mechanisms of gallic acid-induced growth inhibition, apoptosis, and necrosis in hypertrophic scar fibroblasts. *Life Sci*. 2017;179:130–138. doi:10.1016/j.lfs.2016.08.006
18. Chen JY, Zhang L, Zhang H, Su L, Qin LP. Triggering of p38 MAPK and JNK signaling is important for oleanolic acid-induced apoptosis via the mitochondrial death pathway in hypertrophic scar fibroblasts. *Phytother Res*. 2014;28(10):1468–1478. doi:10.1002/ptr.5150
19. Xia W, Wang Q, Lin S, et al. A high-salt diet promotes hypertrophic scarring through TRPC3-mediated mitochondrial Ca2+ homeostasis dysfunction. *Heliyon*. 2023;9(8):e18629. doi:10.1016/j.heliyon.2023.e18629
20. Andrieux P, Chevillard C, Cunha-Neto E, Nunes J. Mitochondria as a cellular hub in infection and inflammation. *Int J Mol Sci*. 2021;22(21):11338. doi:10.3390/ijms222111338
21. Vringer E, Tait S. Mitochondria and cell death-associated inflammation. *Cell Death Differ*. 2023;30(2):304–312. doi:10.1038/s41418-022-01094-w
22. Birney E. Mendelian Randomization. *Cold Spring Harb Perspect Med*. 2022;12(4). doi:10.1101/cshperspect.a041302
23. Ference BA, Holmes MV, Smith GD. Using Mendelian randomization to improve the design of randomized trials. *Cold Spring Harb Perspect Med*. 2021;11(7):a040980. doi:10.1101/cshperspect.a040980
24. Ference BA. Interpreting the clinical implications of drug-target Mendelian randomization studies. *J Am Coll Cardiol*. 2022;80(7):663–665. doi:10.1016/j.jacc.2022.06.007
25. Zhu Z, Zhang F, Hu H, et al. Integration of summary data from GWAS and eQTL studies predicts complex trait gene targets. *Nat Genet*. 2016;48(5):481–487. doi:10.1038/ng.3538
26. McRae AF, Marioni RE, Shah S, et al. Identification of 55,000 replicated DNA methylation QTL. *Sci Rep*. 2018;8(1):17605. doi:10.1038/s41598-018-35871-w

27. Gagliano taliun SA, Evans DM. Ten simple rules for conducting a mendelian randomization study. *PLoS Comput Biol*. 2021;17(8):e1009238. doi:10.1371/journal.pcbi.1009238
28. Skrivankova VW, Richmond RC, Woolf B, et al. Strengthening the reporting of observational studies in epidemiology using mendelian randomization: the STROBE-MR statement. *JAMA*. 2021;326(16):1614–1621. doi:10.1001/jama.2021.18236
29. Rath S, Sharma R, Gupta R, et al. MitoCarta3.0: an updated mitochondrial proteome now with sub-organelle localization and pathway annotations. *Nucleic Acids Res*. 2021;49(D1):D1541–D1547. doi:10.1093/nar/gkaa1011
30. Ferkingstad E, Sulem P, Atlason BA, et al. Large-scale integration of the plasma proteome with genetics and disease. *Nat Genet*. 2021;53 (12):1712–1721. doi:10.1038/s41588-021-00978-w
31. Li X, Liang Z. Causal effect of gut microbiota on pancreatic cancer: a Mendelian randomization and colocalization study. *J Cell Mol Med*. 2024;28 (8):e18255. doi:10.1111/jcmm.18255
32. Finnerty CC, Jeschke MG, Branski LK, Barret JP, Dziewulski P, Herndon DN. Hypertrophic scarring: the greatest unmet challenge after burn injury. *Lancet*. 2016;388(10052):1427–1436. doi:10.1016/S0140-6736(16)31406-4
33. Cai S, Zhao M, Zhou B, et al. Mitochondrial dysfunction in macrophages promotes inflammation and suppresses repair after myocardial infarction. *J Clin Invest*. 2023;133(4). doi:10.1172/JCI159498
34. Wei T, Xu Z. The diagnostic value and associated molecular mechanism study for fibroblast-related mitochondrial genes on keloid. *Skin Res Technol*. 2024;30(9):e70024. doi:10.1111/srt.70024
35. Wang Q, Wang P, Qin Z, et al. Altered glucose metabolism and cell function in keloid fibroblasts under hypoxia. *Redox Biol*. 2021;38:101815. doi:10.1016/j.redox.2020.101815
36. Xiao H, Palhan V, Yang Y, Roeder RG. TIP30 has an intrinsic kinase activity required for up-regulation of a subset of apoptotic genes. *EMBO J*. 2000;19(5):956–963. doi:10.1093/emboj/19.5.956
37. Carbajo-García MC, Corachán A, Juárez-Barber E, et al. Integrative analysis of the DNA methylome and transcriptome in uterine leiomyoma shows altered regulation of genes involved in metabolism, proliferation, extracellular matrix, and vesicles. *J Pathol*. 2022;257(5):663–673. doi:10.1002/path.5920
38. Korntner S, Lehner C, Gehwolf R, et al. Limiting angiogenesis to modulate scar formation. *Adv Drug Deliv Rev*. 2019;146:170–189. doi:10.1016/j.addr.2018.02.010
39. Zhang J, Liu Z, Cao W, et al. Amentoflavone inhibits angiogenesis of endothelial cells and stimulates apoptosis in hypertrophic scar fibroblasts. *Burns*. 2014;40(5):922–929. doi:10.1016/j.burns.2013.10.012
40. Patel AS, Ludwinski FE, Mondragon A, et al. HTATIP2 regulates arteriogenic activity in monocytes from patients with limb ischemia. *JCI Insight*. 2023;8(24). doi:10.1172/jci.insight.131419
41. Ito M, Jiang C, Krumm K, et al. TIP30 deficiency increases susceptibility to tumorigenesis. *Cancer Res*. 2003;63(24):8763–8767.
42. NicAmhlaoibh R, Shtivelman E. Metastasis suppressor CC3 inhibits angiogenic properties of tumor cells in vitro. *Oncogene*. 2001;20(2):270–275. doi:10.1038/sj.onc.1204075
43. Hinz B, Lagares D. Evasion of apoptosis by myofibroblasts: a hallmark of fibrotic diseases. *Nat Rev Rheumatol*. 2020;16(1):11–31. doi:10.1038/s41584-019-0324-5
44. Li Q, Zhang B, Lu J, et al. SNHG1 functions as a ceRNA in hypertrophic scar fibroblast proliferation and apoptosis through miR-320b/CTNNB1 axis. *Arch Dermatol Res*. 2023;315(6):1593–1601. doi:10.1007/s00403-022-02516-y
45. Shi J, Xiao H, Li J, et al. Wild-type p53-modulated autophagy and autophagic fibroblast apoptosis inhibit hypertrophic scar formation. *Lab Invest*. 2018;98(11):1423–1437. doi:10.1038/s41374-018-0099-3
46. Wynn TA, Ramalingam TR. Mechanisms of fibrosis: therapeutic translation for fibrotic disease. *Nat Med*. 2012;18(7):1028–1040. doi:10.1038/nm.2807
47. Zhao X, Kwan J, Yip K, Liu PP, Liu FF. Targeting metabolic dysregulation for fibrosis therapy. *Nat Rev Drug Discov*. 2020;19(1):57–75. doi:10.1038/s41573-019-0040-5
48. Moretti L, Stalfort J, Barker TH, Abebayehu D. The interplay of fibroblasts, the extracellular matrix, and inflammation in scar formation. *J Biol Chem*. 2022;298(2):101530. doi:10.1016/j.jbc.2021.101530
49. Igota S, Tosa M, Murakami M, et al. Identification and characterization of Wnt signaling pathway in keloid pathogenesis. *Int J Med Sci*. 2013;10 (4):344–354. doi:10.7150/ijms.5349
50. Meng X, Gao X, Shi K, et al. Interferon-α2b-induced RARRES3 upregulation inhibits hypertrophic scar fibroblasts' proliferation and migration through Wnt/β-catenin pathway suppression. *J Interferon Cytokine Res*. 2023;43(1):23–34. doi:10.1089/jir.2022.0183
51. Tan Y, Zhang M, Kong Y, et al. Fibroblasts and endothelial cells interplay drives hypertrophic scar formation: insights from in vitro and in vivo models. *Bioeng Transl Med*. 2024;9(2):e10630. doi:10.1002/btm2.10630
52. Yuan Q, Tang B, Zhang C. Signaling pathways of chronic kidney diseases, implications for therapeutics. *Signal Transduct Target Ther*. 2022;7 (1):182. doi:10.1038/s41392-022-01036-5
53. Zhang T, Wang XF, Wang ZC, et al. Current potential therapeutic strategies targeting the TGF-β/Smad signaling pathway to attenuate keloid and hypertrophic scar formation. *Biomed Pharmacother*. 2020;129:110287. doi:10.1016/j.biopha.2020.110287
54. Xiaojie W, Banda J, Qi H, et al. Scarless wound healing: current insights from the perspectives of TGF-β, KGF-1, and KGF-2. *Cytokine Growth Factor Rev*. 2022;66:26–37. doi:10.1016/j.cytogfr.2022.03.001
55. He T, Bai X, Jing J, et al. Notch signal deficiency alleviates hypertrophic scar formation after wound healing through the inhibition of inflammation. *Arch Biochem Biophys*. 2020;682:108286. doi:10.1016/j.abb.2020.108286
56. Li B, Gao C, Diao JS, et al. Aberrant Notch signalling contributes to hypertrophic scar formation by modulating the phenotype of keratinocytes. *Exp Dermatol*. 2016;25(2):137–142. doi:10.1111/exd.12897
57. Ouyang H, Gore J, Deitz S, Korc M. microRNA-10b enhances pancreatic cancer cell invasion by suppressing TIP30 expression and promoting EGF and TGF-β actions. *Oncogene*. 2014;33(38):4664–4674. doi:10.1038/onc.2013.405
58. Brosnan CF, John GR. Revisiting Notch in remyelination of multiple sclerosis lesions. *J Clin Invest*. 2009;119(1):10–13. doi:10.1172/JCI37786
59. Hua Y, Bergers G. Tumors vs. chronic wounds: an immune cell's perspective. *Front Immunol*. 2019;10:2178. doi:10.3389/fimmu.2019.02178
60. Zheng N, Wei J, Wu D, Xu Y, Guo J. Master kinase PDK1 in tumorigenesis. *Biochim Biophys Acta Rev Cancer*. 2023;1878(6):188971. doi:10.1016/j.bbcan.2023.188971

61. Kim JW, Tchernyshyov I, Semenza GL, Dang CV. HIF-1-mediated expression of pyruvate dehydrogenase kinase: a metabolic switch required for cellular adaptation to hypoxia. *Cell Metab*. 2006;3(3):177–185. doi:10.1016/j.cmet.2006.02.002
62. Tian L, Wu D, Dasgupta A, et al. Epigenetic metabolic reprogramming of right ventricular fibroblasts in pulmonary arterial hypertension: a pyruvate dehydrogenase kinase-dependent shift in mitochondrial metabolism promotes right ventricular fibrosis. *Circ Res*. 2020;126 (12):1723–1745. doi:10.1161/CIRCRESAHA.120.316443
63. Kim J, Kim HS, Choi DH, et al. Kaempferol tetrasaccharides restore skin atrophy via PDK1 inhibition in human skin cells and tissues: bench and clinical studies. *Biomed Pharmacother*. 2022;156:113864. doi:10.1016/j.biopha.2022.113864
64. Jia S, Agarwal M, Yang J, Horowitz JC, White ES, Kim KK. Discoidin domain receptor 2 signaling regulates fibroblast apoptosis through PDK1/ Akt. *Am J Respir Cell Mol Biol*. 2018;59(3):295–305. doi:10.1165/rcmb.2017-0419OC
65. Eming SA, Wynn TA, Martin P. Inflammation and metabolism in tissue repair and regeneration. *Science*. 2017;356(6342):1026–1030. doi:10.1126/ science.aam7928
66. Short WD, Wang X, Li H, et al. Interleukin-10 producing T lymphocytes attenuate dermal scarring. *Ann Surg*. 2021;274(4):627–636. doi:10.1097/ SLA.0000000000004984
67. Huang Y, Feng Q, Zhang Y, et al. The effect of PDK1 in maintaining immune cell development and function. *Biochem Biophys Res Commun*. 2024;721:150106. doi:10.1016/j.bbrc.2024.150106
68. Yu M, Owens DM, Ghosh S, Farber DL. Conditional PDK1 ablation promotes epidermal and T-cell-mediated dysfunctions leading to inflammatory skin disease. *J Invest Dermatol*. 2015;135(11):2688–2696. doi:10.1038/jid.2015.232
69. Zuo Q, He J, Zhang S, et al. PPARγ coactivator-1α suppresses metastasis of hepatocellular carcinoma by inhibiting warburg effect by PPARγ-Dependent WNT/β-Catenin/pyruvate dehydrogenase kinase isozyme 1 axis. *Hepatology*. 2021;73(2):644–660. doi:10.1002/hep.31280
70. Lee M, Chen GT, Puttock E, et al. Mathematical modeling links Wnt signaling to emergent patterns of metabolism in colon cancer. *Mol Syst Biol*. 2017;13(2):912. doi:10.15252/msb.20167386
71. Han X, Wei Y, Wu X, Gao J, Yang Z, Zhao C. PDK1 regulates transition period of apical progenitors to basal progenitors by controlling asymmetric cell division. *Cereb Cortex*. 2020;30(1):406–420. doi:10.1093/cercor/bhz146
72. Kelly AP, Finlay DK, Hinton HJ, et al. Notch-induced T cell development requires phosphoinositide-dependent kinase 1. *EMBO J*. 2007;26 (14):3441–3450. doi:10.1038/sj.emboj.7601761
73. Sun Z, Yao Y, You M, et al. The kinase PDK1 is critical for promoting T follicular helper cell differentiation. *Elife*. 2021;10. doi:10.7554/eLife.61406
74. Macdonald IA, Bennett T, Fellows IW. Catecholamines and the control of metabolism in man. *Clin Sci*. 1985;68(6):613–619. doi:10.1042/ cs0680613
75. Zhao X, Luo J, Huang Y, et al. Injectable antiswelling and high-strength bioactive hydrogels with a wet adhesion and rapid gelling process to promote sutureless wound closure and scar-free repair of infectious wounds. *ACS Nano*. 2023;17(21):22015–22034. doi:10.1021/acsnano.3c08625
76. Sha Q, Wang Y, Zhu Z, et al. A hyaluronic acid/silk fibroin/poly-dopamine-coated biomimetic hydrogel scaffold with incorporated neurotrophin-3 for spinal cord injury repair. *Acta Biomater*. 2023;167:219–233. doi:10.1016/j.actbio.2023.05.044
77. Oh J, Fernando A, Muffley L, Honari S, Gibran NS. Correlation between the warrior/worrier gene on post burn pruritus and scarring: a prospective cohort study. *Ann Surg*. 2022;275(5):1002–1005. doi:10.1097/SLA.0000000000004235
78. Qin G, Sun Y, Guo Y, Song Y. PAX5 activates telomerase activity and proliferation in keloid fibroblasts by transcriptional regulation of SND1, thus promoting keloid growth in burn-injured skin. *Inflamm Res*. 2021;70(4):459–472. doi:10.1007/s00011-021-01444-3
79. Wang X, Chu J, Wen CJ, et al. Functional characterization of TRAP1-like protein involved in modulating fibrotic processes mediated by TGF-β/ Smad signaling in hypertrophic scar fibroblasts. *Exp Cell Res*. 2015;332(2):202–211. doi:10.1016/j.yexcr.2015.01.015
80. Mustafa R, Mens MMJ, Van Hilten A, et al. A comprehensive study of genetic regulation and disease associations of plasma circulatory microRNAs using population-level data, Genome. *Biol*. 2024;25(1):276.
81. Chen Y, Zhang Z, Chen Y, et al. Investigating the shared genetic links between hypothyroidism and psychiatric disorders: a large-scale genomewide cross-trait analysis. *J Affect Disord*. 2025;369:312–320. doi:10.1016/j.jad.2024.08.202